The Phases of Argon
Periodic Boundary Conditions Simulation Studies

Ethan van Woerkom*

28/03/2019

Abstract

A simulation of Argon with a Lennard-Jones interaction potential and periodic boundary conditions is presented. Design stayed close to original design document, with improvements including C++ accelerated forces calculations, giving thirty-fold speed-up, and additional analysis code for creating phase diagrams and calculating diffusion constants from multiple simulation trials. Radial Distribution Functions and Mean Square Displacement diagrams for the three phases of Argon are calculated and discussed. Special limiting properties of Mean Square Displacement and Radial Density Function diagrams are derived, discussed and verified. Diffusion constants of $7.5(3) \times 10^{-5} \mathrm{cm}^2 \mathrm{s}^{-1}$ for fluid Argon and $6.05(5) \times 10^{-4} \mathrm{cm}^2 \mathrm{s}^{-1}$ for Argon gas are calculated. Preliminary Argon phase diagrams are presented. Using these, and other results, the shortcomings of this simulation technique are critiqued and improvements suggested.
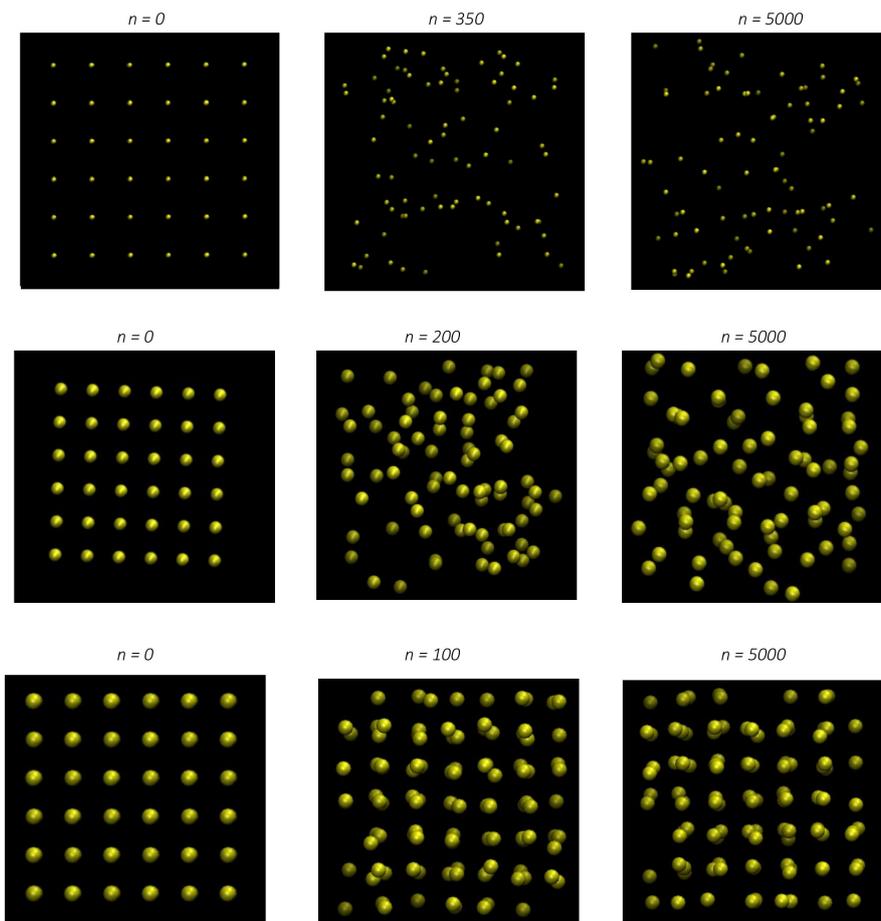
Figure 1: Visualisation of, from top to bottom: Argon gas, Argon fluid, Argon solid phases[1].

---

*Simulation and analysis done in equal parts with C. Kourris.

Constant	MD-Units Value	Equivalent SI Units
ϵ_{Argon}	1	1.65×10^{-21} J [2]
σ_{Argon}	1	3.405×10^{-8} cm[2]
m_{Argon}	1	6.632×10^{-23} g [2]
k_b	1	1.3807×10^{-23} JK^{-1} [3]
Quantity	**MD-Units**	**SI Units**
Length L^*	σ_{Argon}	3.405×10^{-8} cm[2]
Time T^*	$\sigma_{Argon}\sqrt{m_{Argon}/\epsilon_{Argon}}$	2.16×10^{-12} s
Energy E^*	ϵ_{Argon}	1.65×10^{-21} J
Mass m^*	m_{Argon}	6.632×10^{-23} g [2]
Temperature T^*	ϵ_{Argon}/k_b	119.8 K
Diffusion Rate D^*	$\sigma\sqrt{\epsilon_{Argon}/m_{Argon}}$	5.37×10^{-4} cm$^2s^{-1}$
Specific Volume V^*	σ^3	23.77cm^3 mol^{-1}

Table 1: Units and constants reference.

I Introduction

This report investigates the properties of the three phases of molecular Argon using numerical simulations. General properties such as the radial distribution function and mean square displacement of Argon are presented. Using this the diffusion constant of the solid and gas phases is calculated. Finally we present an elementary phase diagram of Argon derived from simulations.

Sec. II presents the methods, layout and algorithms of the simulation. Sec. III presents the results. In Sec. IV discusses the quality and shortcomings of the data. In Sec. V we peer-review code. Finally in Sec. VI we summarise and autopsy the project.

II Method

II.1 Overview of Simulation

Argon atoms act as point particles, with corresponding Lennard-Jones (LJ) potentials (Eq. 1), representing the neutral inter-atomic interactions. N atoms are initialised in a simulation box in an FCC configuration, the configuration of solid Argon. The initialisation is dictated by the number of particles N, the number density n, and the temperature T. For a complete FCC lattice it is preferred that $N = 4U^3$, where U represents the number of unit cells per side. The N atoms are assigned random velocites according to the Maxwell-Boltzmann distribution at temperature T.

$$V(r) = 4\epsilon\left[\left(\frac{\sigma}{r}\right)^{12} - \left(\frac{\sigma}{r}\right)^6\right] \tag{1}$$

The simulation is started and conducted using the second-order Verlet integration scheme. The simulation utilises periodic boundary conditions (PBC), so particles may move freely through one side of the simulation box and emerge at the opposing side. The minimum-image-convention (MIC) is respected, stipulating that particles only interact with the nearest image of a neighbour, as a neighbouring molecule may be reached through several directions. Finally to reduce computational load, particles may only interact up to a certain cutoff-distance, beyond which the Lennard-Jones potential is neglected and set to zero.

II.2 Units

The simulation uses "Molecular Dynamics Units" (MDU), implying that the LJ-parameters ϵ, σ for Argon, as well as the atomic mass m and the Boltzmann constant, k_b, are set to 1. Using dimensional analysis the units of other quantities may be derived (Table 1). Unless explicitly stated, these units are the default in this paper.

II.3 Simulation Settings

The settings in Table 2 were chosen to represent the three different phases of Argon.

$N_{particles} = 108$ was chosen to encourage the stability of the crystalline solid phase in Argon, whereas $N_{particles} = 80$ was chosen to encourage melting for the fluid and gaseous phases. See Fig. 1 for a visualisation.

Phase	N	LJ-Cutoff	Density	T (MD)	Length (steps)	V_m (cm^{3}mol^{-1})	T (K)
Solid	108	2.5	0.85	0.626	10000	28.0	75
Fluid	80	2.5	0.486	1.169	10000	49.0	140
Gas	80	3.5	0.02125	1.544	10000	1119	185.0

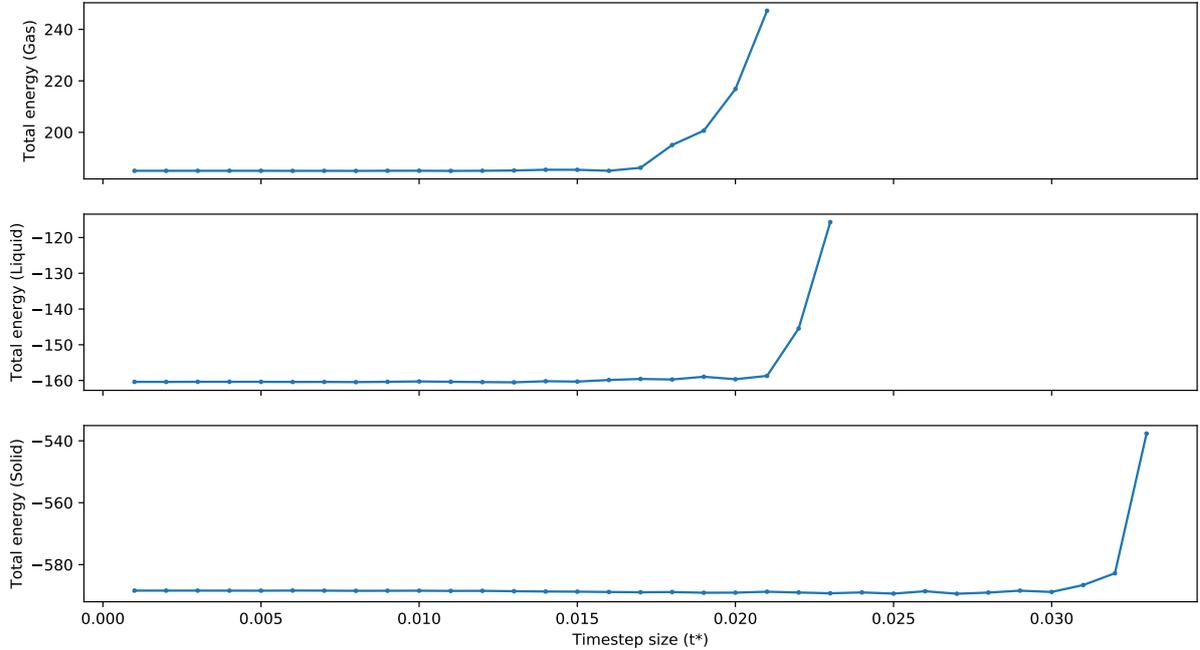Table 2: Simulation specifications

Figure 2: System total energy for a solid, liquid, and gas.
Measured after 10,000 timesteps, as a function of timestep size.

II.4   Description of Program and Algorithm

The simulation was implemented using Python 3. An object-oriented, abstracted approach was chosen. The class "Partice3D" represented individual particles. The class "Box" aggregated these particles and the properties of a simulation into a single object. The get_forces method of the Box class calculated the force for each unique particle pair, halving computational load by using Newton's Third Law. Realising this was the Achilles heel of the simulation, with a complexity of $O(N^2)$, we decided to boost this method and reimplement it in C++. Simulation times were reduced from ~20 min. to ~40s for a 10,000 step simulation.

II.5   Timestep and Equilibration Time

Energies were determined for simulations of 10,000 timesteps, whilst varying timestep size (Fig. 2). Timesteps of up to 0.015 were found to be well-behaved, however a timestep of 0.005 was chosen to increase precision and reliability throughout all simulations.

The energy equilibration time was also determined to get an indication of when "average" behaviour begins. System total, potential, and kinetic energies are plotted as a function of time in Fig. 3 for the different phases of Argon. As is visible, energies equilibrated completely within approximately 1 units of time, which corresponds to 200 timesteps. Behaviour after 1000 timesteps may therefore be taken to be fully representative for Argon in equilibrium.
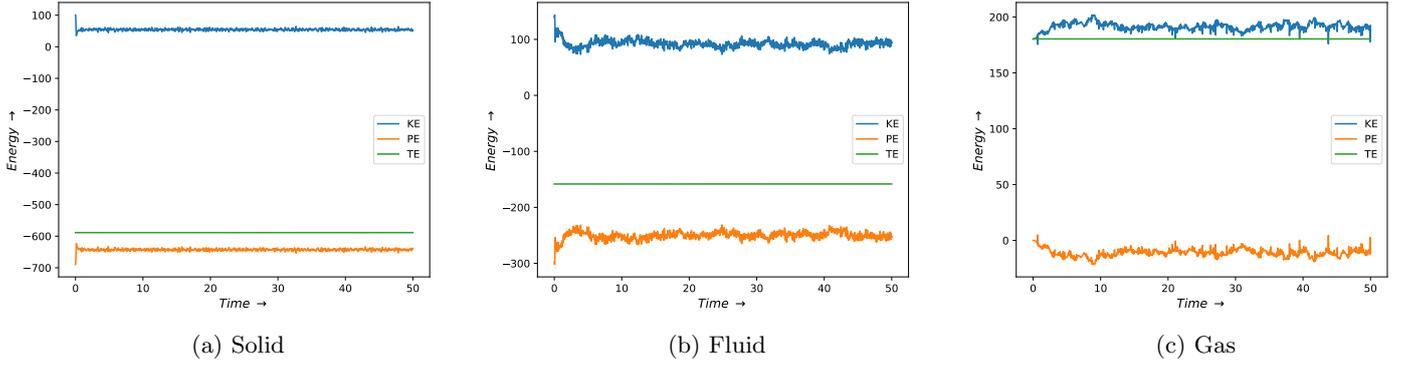
| (a) Solid | (b) Fluid | (c) Gas |

Figure 3: Various phases of Argon (a-c):
Kinetic, Potential, and Total Energies as function of time.

III   Results

III.1   Radial Distribution Function

Radial distribution functions (RDF) were acquired for the different phases of Argon (Fig. 4a-4c), using Eq. 2 as an approximation to the RDF:

$$\text{RDF}(r) \equiv \frac{1}{N\rho}\langle\sum_{i,j}\delta(r_{ij}-r)\rangle \approx \frac{\#(r_{ij}\in[r,r+dr])}{4\pi r^2 N\rho dr}. \tag{2}$$

A histogram was used to count the unique distance pairs per interval and then normalised appropriately. The radial density function was calculated by running the respective simulations for each phase for 10,000 steps and then averaging the RDF function over the last 200.

III.2   Mean Square Displacement

Mean Square Displacement (MSD) is a measure for the amount of diffusion of the individual atoms in a substance. It is calculated using Eq. 3. MSD, at long times in large systems, grows as Eq. 4. The MSD was calculated for all phases and is displayed in Figs. 4d-4f.

$$\text{MSD}(t) \equiv \left\langle |\mathbf{r}(t)-\mathbf{r}(0)|^2 \right\rangle \tag{3}$$

$$\text{MSD}(t) = 6Dt \tag{4}$$

.

III.3   Diffusion Constant

The diffusion constant D for the fluid and gas may be determined using Eq. 4. Specific simulations were set up to measure this optimally. A set of 10 simulations of length 20.000 timesteps were conducted for either phase. PBC were removed to permit free diffusion with linear growth for long times, with particles physically remaining in the box, but their coordinates changing freely. For each simulation, the MSD was calculated from the start time. A linear fit $\text{MSD}(t) = 6Dt$ was then conducted on timesteps 10.000-20.000 to ensure that the measurement is in the linear regime. The retrieved diffusion constants were then averaged (Table 3). These values are representative for fluid and liquid Argon at the conditions specified in Table 2.

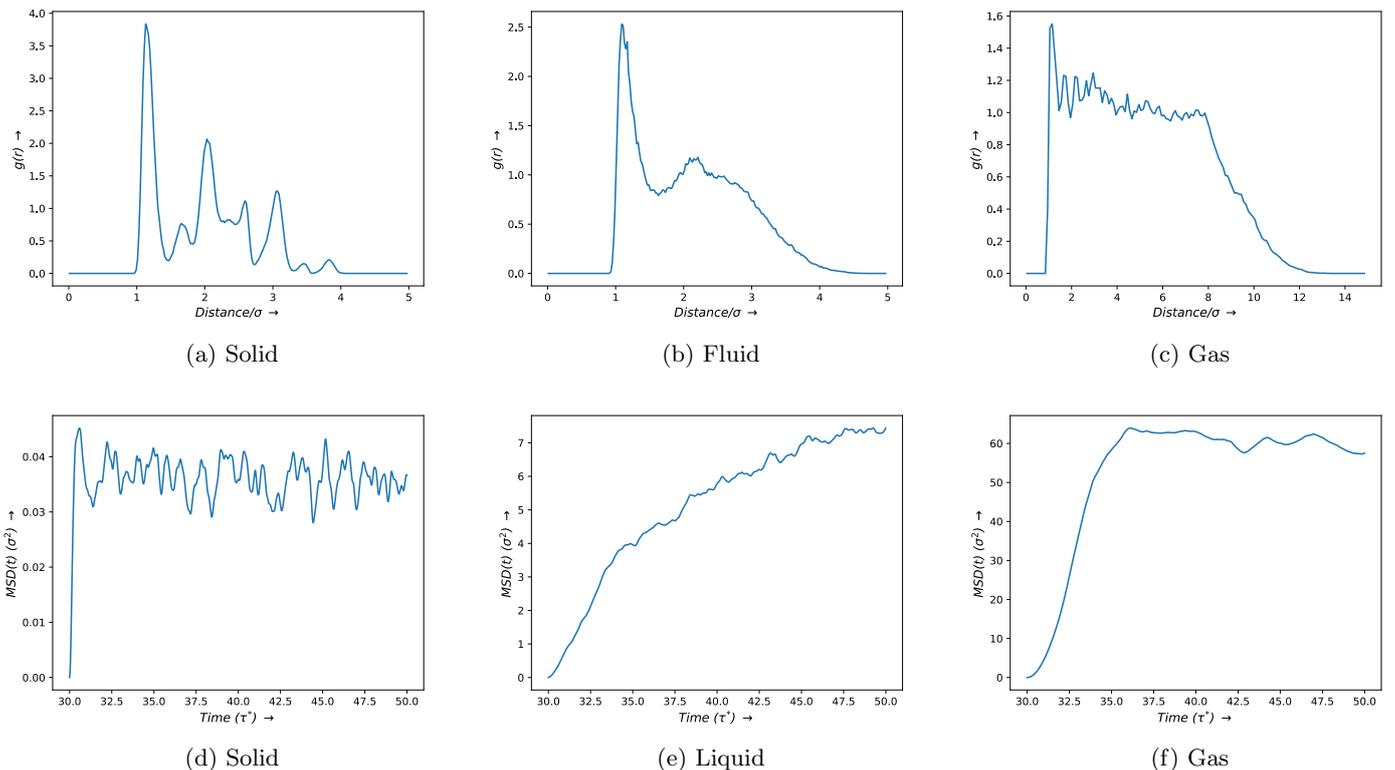| Substance	D (MDU)	Error (MDU)	D (cm²s⁻¹)	Error (cm²s⁻¹)
Fluid	0.139	0.005	7.5×10^{-5}	0.3×10^{-5}
Gas	1.13	0.010	6.05×10^{-4}	0.05×10^{-4}

Table 3: Numerical Diffusion Constant Results

Figure 4: Displayed for various phases of Argon:
(a-c) Radial Distribution Functions, (d-f) Mean Square Displacement Diagrams.

III.4 Phase Diagram

Finally, using simulations with 108 particles, a preliminary phase diagram of Argon was constructed illustrating the solid to fluid/gas phase boundary. 900 simulations of length 2500 timesteps were run in the temperature range of $T = [0.1, 2.5]$ and specific volume range $V = [0.8, 1.8]$, with ranges incremented over 30 steps. MSDs were calculated over the range of 2000-2500 timesteps for each simulation. Examination of the histogram distribution of the maximum MSD attained in each simulation demonstrated the existence of a solid phase with $MSD < 0.1$, intermediate "partially melted" phases in the range $0.1 < MSD < 0.2$, and fluid/gaseous, non-solid phases beyond this range. These are all marked in Fig. 5a. The same was repeated with 80 particles, see Fig. 5b.

IV Discussion

IV.1 Radial Density Function

As is visible the solid (Fig. 4a) clearly has long-range order corresponding to Argon's crystalline structure, with highly structured peaks. The fluid also has a nearest neigbhour peak, then an 'empty site', followed by a second coordination peak, after which the distribution flattens off. The gas only has a small peak on an otherwise flat distribution, reflecting the fact that gas particles are largely uncorrelated except for occasional collisions. All RDFs begin to decay for r larger than $a/2$, where a is the box dimension, as beyond this, MIC specifies that neighbours are no longer all unique ($r_d = 2.51$ for solid, $r_d = 2.74$ for liquid, $r_d = 7.78$ for gas). Thus the density drops off until it reaches zero at $r = \frac{\sqrt{3}a}{2}$, the maximum separation possible between two particles ($r_0 = 4.35$ for solid, $r_0 = 4.75$ for liquid, $r_0 = 13.5$ for gas). The RDF diagrams derived for Argon thus agree with our expectations.

IV.2 MSD and Diffusion constant

As is visible in Fig. 4d, the MSD for a solid rapidly reaches a small equilibrium value, indicating mean displacements much smaller than the lattice spacing.

The fluid on the other hand displays a steady linear growth trend, in agreement with the diffusion equation, which then flattens off as molecules become maximally diffused and reach the maximal displacement permitted by the size of the box.
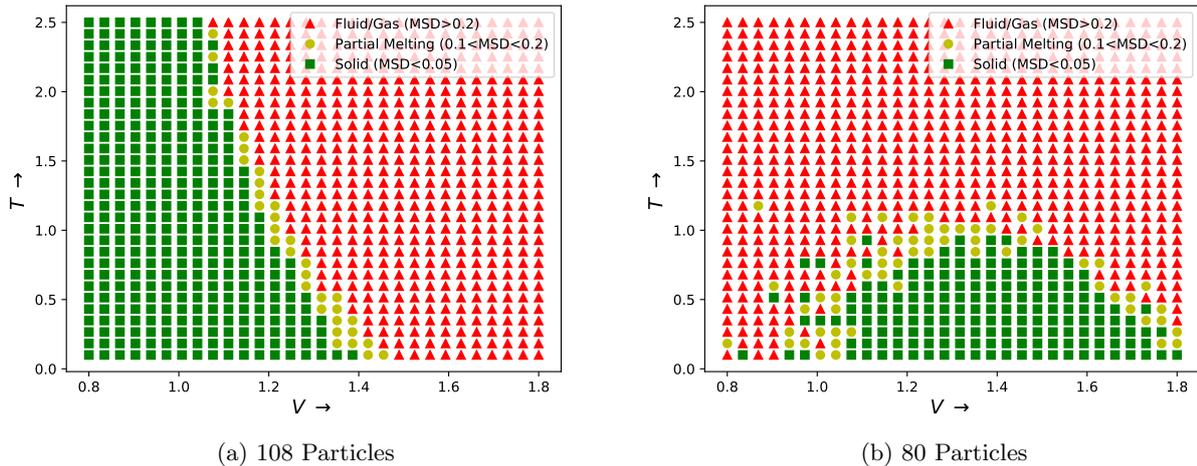
(a) 108 Particles   (b) 80 Particles

Figure 5: Argon phase diagrams each produced from aggregate of 900 simulations.

The gas initially shows quadratic growth as for small distances interactions are minimal and thus: $\mathrm{MSD}(t) = \sum_i |\mathbf{r}_i(t) - \mathbf{r}_i(0)|^2 = \sum_i |\mathbf{r}_i(0) + \mathbf{v}_i(0)t - \mathbf{r}_i(0)|^2| = t^2 \sum_i |\mathbf{v}_i(0)|^2$.

A long-term limit of $a^2/4$ for the MSD in a large box of dimension a may be derived (Eq. 5). This assumes that eventually the particle probability is equal everywhere. The gas and fluid have box sizes 15.56 and 5.48 respectively which gives limits of 7.5 and 60.5 for the MSD, which agree.

$$\lim_{t \to \infty} \mathrm{MSD}(t) = \iiint_{Box} r^2 p(x, y, z) dx dy dz = \iiint_{Box} \frac{x^2 + y^2 + z^2}{V} dx dy dz$$

$$= \frac{3}{a^3} \iiint_{Box} x^2 dx dy dz = \frac{3}{a} \left| \frac{x^3}{3} \right|_{-\frac{a}{2}}^{\frac{a}{2}} = \frac{a^2}{4}. \quad (5)$$

Literature suggests diffusion constants in the range of $20.4 - 21.3 \times 10^{-5}$ cm^{2}s^{-1}[4] for fluid Argon at ($V_m = 57.45$ cm^{3}mol^{-1}, T = 157 K), which is approximately three times larger value than our results with roughly similar conditions. The larger molar volumes and temperatures of this value, and more importantly, a lower than nominal temperature in our simulation (see Sec. IV.4) likely contributed to this difference. Gas experimental values are rare, but may be compared with the theoretical value of $D = 1.12$ derived from (Eq. 6 [5], with estimated particle diameter $d = 2.5$, yielding extremely close agreement (1% difference).

$$D = \frac{\lambda}{3} \langle v \rangle = \frac{1}{3\sqrt{2}\sigma n} \left(\frac{8 k_b T}{\pi m} \right)^{\frac{1}{2}} = \frac{1}{d^2 n} \left(\frac{4 k_b T}{9\pi^3 m} \right)^{\frac{1}{2}}. \quad (6)$$

IV.3 Argon Phase Diagram

The Argon phase diagram illlustrates the shortcomings of the simulation. The small simulation box with periodic boundary conditions severely handicaps the study of the phases of Argon for the following reasons:

- The filled FCC 108-particle lattice used in the simulation induces superheating (Fig. 5a), the presence of the solid phase appearing when melting is in fact preferred. The small box size requires melting to happen at all points simultaneously to break the lattice. In reality however, melting happens at a boundary. Melting is thus unlikely to happen within the timescale of a simulation. Thus melting appears in simulation at much higher temperatures. The triple point of Argon ($V = 1.04, T = 0.70$) shows this. In the diagram, it should be at the phase boundary, but is surrounded in the solid phase. An incomplete FCC lattice using 80 particles was tested, showing melting at much lower temperatures.

- The temperatures in the simulations are incorrect. See Sec.IV.4.

- This is a constant (V, E) simulation, contrary to common experimental (T, P) conditions. At constant V, two coexisting phases may be energetically favourable. Due to the small size of the simulation box, that is prevented, thus the simulation is unrealistic at volumes where two phases should be coexisting.

6

Phase	T_{begin}(MDU)	T_{end}(MDU)
Solid	1.544	1.620
Fluid	1.169	0.795
Gas	0.626	0.335

Table 4: Simulation beginning and end temperatures.

Longer simulation times would give a more equilibrated picture. Secondly, calculating the MSD for a longer portion of the simulation would increase the MSD value for the liquid and gas, thus making them easier to distinguish from the solid phase. Finally, increasing particle number would also give more realistic melting. These measures would improve the diagram quality but increase simulation time beyond the current 4 hours.

IV.4 Simulation Temperature

An important weakness of the simulation is non-constant temperatures. At the end of each simulation, the (kinetic) temperatures were calculated with $T = \frac{2E_{ktot}}{3N}$. Table 4 shows how the temperatures changed across the simulation. As described in Sec. II.1, only the kinetic degrees of freedom were initialised with energies corresponding to the temperature. In the solid there are however 3 kinetic + 3 potential degrees of freedom, explaining the halving of the temperature. In the fluid this is less severe since there are no distinctly separable potential degrees of freedom. In the gas the temperature slightly increases, since for large distances, a decrease in inter-atomic distance results in a decrease in Lennard-Jones potential and thus increased kinetic energy. These results therefore show that the temperatures used in the simulations are untrustworthy. This should be taken into acccount in future work.

V Code Peer-Review

We now peer-review an alternative implementation of this Argon Simulation.

The program layout is good with modules organising the code. Comments and clear naming conventions convey the working and intention of the code well.

The main function is still too large and could have been split into functions, e.g. a separate simulation function. A class is used to facilitate storing and handling individual particles. Further use of object-orientation would have simplified the variables presented to the user in the main function. This would all increase ease of use and code flexibility.

The program uses MD units but requires SI units from the end-user, adding complexity, as data analysis is done in MD units again. Additionally, the program does not run as-is, and does not have preset inputs ready, but must be called with all variables from the Python console, which also reduces ease.

The simulated physics was accurate, as far as verifiable matching our results. Only a Lennard-Jones potential cutoff was lacking, but as this is a performance optimisation it is not critical.

Performance was good. A 1000 timestep simulation and analysis of the solid configuration took 211s, whereas in our Python implementation this took 422s, of which 392s for simulation.

VI Conclusion and Post-Mortem

We have presented a numerical simulation of Argon, and studied its different phases. We produced RDF, MSD and phase diagrams for Argon fluid and gas. We measured diffusion constants of $7.5(3) \times 10^{-5}$cm^{2}s^{-1} for Argon fluid and $6.05(5) \times 10^{-4}$cm^{2}s^{-1} for Argon gas. The discussion has raised many improvement points. The overall way forward is to repeat this analysis with a simulation using a heat bath and implementing constant pressure conditions in a larger system. Another possibility would be to calculate constant volume heat capacities by using more appropriate temperature measures, and varying E. The use of quantum methods would be more accurate for deriving values such as heat capacities, but can not replace the use of Molecular Dynamics for diffusion studies.

All analyses and simulations were done jointly with C. Kourris. This went very smoothly. Teamwork was good from the start, both spotting bugs in each other's code, and Git combined with early and thorough code structure and algorithm planning greatly facilitated this. Accelerating in C++ has been a pleasure since it permitted us to do analyses far beyond the normal material. We would not implement the program significantly differently if we did this again.

References

[1] Humphrey, W., Dalke, A. and Schulten, K., *"VMD - Visual Molecular Dynamics"*, J. Molec. Graphics, 1996, vol. 14, pp. 33-38.

[2] Miguel Martinez-Canales, *"Project B: Phase Diagram of Argon"*, Document from University of Edinburgh Computer Modelling 2018-2019 Course Page.

[3] G. Verkerk et al., *"BINAS English Edition: Handbook for the natural sciences and mathematics"*, Wolters-Noordhoff (2007).

[4] R. A. Fisher and R. O. Watts, *"Calculated Self-Diffusion Coefficients for Liquid Argon"*, Aust. J. Phys., 1972, 25, 529-38.

[5] S. Titmuss and S. McWilliams, *"Physics of Matter: Kinetic Theory of Gases"*, Course Handbook of Edinburgh University taught course (2018).

[6] J.D. Hunter, *"Matplotlib: A 2D graphics environment"*, Computing In Science & Engineering, Vol. 9 No. 3, pages 90-95 (2007).